



CRONO: a fast and reconfigurable macro X-ray fluorescence scanner for in-situ investigations of heritage objects

Journal:	<i>X-Ray Spectrometry</i>
Manuscript ID	XRS-16-0094
Wiley - Manuscript type:	Research Article
Date Submitted by the Author:	27-Sep-2016
Complete List of Authors:	<p>Alberti, Roberto; XGLab S.R.L, Frizzi, Tommaso; XGLab s.r.l. Bombelli, Luca; XGLab s.r.l. , Gironda, Michele; XGLab S.R.L, Aresi, Nicola; XGLab s.r.l. , Rosi, Francesca; Istituto di Scienze e Tecnologie Molecolari - CNR, via Elce di Sotto 8, 06123, Perugia, Italy Miliani, Costanza; Istituto di Scienze e Tecnologie Molecolari - CNR, via Elce di Sotto 8, 06123, Perugia, Italy Tranquilli, Gloria; Istituto Superiore per la Conservazione ed il Restauro – ISCR, Roma , Italy Talarico, Fabio; Istituto Superiore per la Conservazione ed il Restauro – ISCR, Roma , Italy Cartechini, Laura; Istituto di Scienze e Tecnologie Molecolari - CNR, via Elce di Sotto 8, 06123, Perugia, Italy</p>
Keywords:	macro XRF, portable XRF, elemental distribution images, paintings

SCHOLARONE™
Manuscripts

CRONO: a fast and reconfigurable macro X-ray fluorescence scanner for in-situ investigations of heritage objects

R. Alberti (1), T. Frizzi (1), L. Bombelli (1), M. Gironda (1), N. Aresi (1), , F. Rosi (2), C. Miliani (2), G. Tranquilli (3), F. Talarico (3), L. Cartechini (2)

1 XGLab SRL, via Francesco D'Ovidio 3, I-20131, Milano, Italy, email: info@xglab.it

2 Istituto di Scienze e Tecnologie Molecolari - CNR, via Elce di Sotto 8, 06123, Perugia, Italy

3 Istituto Superiore per la Conservazione ed il Restauro – ISCR, Roma , Italy

Abstract

CRONO is a new portable and easy reconfigurable macro X-ray fluorescence (MA-XRF) scanner based on the energy dispersive X-ray fluorescence technique, which has been specifically designed for in-situ, fast and non-invasive elemental mapping. The main components are fully integrated into the measurement head which includes an X-ray tube, a large area silicon drift detector, a microscope camera, two pointing lasers, a He purging set, and fast acquisition electronics. This very compact head is mounted on motorized stages (with a linear speed up to 45mm/s) that allow the scanning of areas up to 45×60cm². Three collimators (0.5mm, 1mm and 2mm diameter) are software selectable to obtain different spot-sizes on the sample. The typical measurement time for the full scanned area ranges from 1h with the 2mm collimator to about 15h with the 0.5mm collimator using a dwell time of 50ms. Technical details and achievable performances of the instrument are presented and discussed along with an example of application which illustrates the value of the developed instrument in the investigation of paintings.

Keywords: macro XRF, portable XRF, elemental distribution images, paintings

Introduction

X-ray fluorescence spectroscopy is a long established technique for non invasive in situ elemental analysis of heritage objects [1]. In most of the analytical applications, the compositional heterogeneity of heritage materials poses high challenges especially for paintings and, more in general, for polychrome surfaces. In order to reveal not only the composition but also the distribution of painting materials and thus the artist's working method, the use of chemical imaging techniques at the macro-scale and with high-spatial resolution is extremely valuable. In order to achieve these purposes in the last years the use of XRF for elemental macro scale mapping of paintings at high spatial resolution was rapidly increasing with rising success [2-5]. The technique provides (sub-)surface non-invasive analysis of painted artefacts ([6] and references therein) and a deep insight into painting materials especially when combined with complementary imaging techniques [7-8].

Until recent times, micro- and macro- XRF mapping/imaging analysis was possible only by synchrotron radiation requiring the transport of precious artworks to large scale facilities [9- 11]. Only in the very last years the advancement in instrumental technologies has made it possible to transpose the technique to laboratory and to in-situ applications [2, 3, 12, 13]. However finding a good compromise which takes into account instrument portability, large scans, beam dimension, count rates, and acquisition time is still very challenging [2, 14, 15].

In this paper, we present CRONO, a new commercial reconfigurable MA-XRF scanner implemented by XGLab (Milan, Italy) in collaboration with ISTM-CNR. CRONO is fully portable, it scores state of the art analytical performances, and has been specifically designed for applications in cultural heritage in order to meet the high demanding analytical requirements for use in the mobile laboratory MOLAB [16]. On the basis of the MOLAB decennial experience on non-invasive in-situ investigations of artworks, full portability, easy reconfiguration, and fast acquisitions are requisites indispensable for "in field" studies of heritage materials. In the following, a detailed description of CRONO and of its analytical characteristics is given. Furthermore, as applicative example, results from the analysis of a historical painting are presented and discussed in order to illustrate the value of the instrument in heritage science.

Instrument and technical characteristics

A general view of CRONO in some of the possible configurations is shown in Fig.1. XRF components are fully integrated into a compact ($30 \times 16 \times 15 \text{cm}^3$) and light (3kg) detection head mounted on a motorised XYZ stage. The excitation source is a highly efficient and compact 10W

1
2
3 X-ray tube generator with Rh anode (tube voltage and current are selectable from 10 to 50kV and
4 form 5 to 200 μ A, respectively); the X-ray detector element is a large area (active collimated area is
5 50mm²) SDD (Silicon Drift Detector) equipped with CUBE preamplifier (a CMOS circuit provided
6 by XGLab [17]). Such X-ray detection module is characterised by state-of-the-art performances.
7
8 The detection module is read-out by a new digital pulse processor (named DANTE and developed
9 by XGLab) characterised by excellent noise and high count-rate performances, and real-time data
10 transmission capability for on-the-flight data collection [18]. The complete spectra information is
11 saved and made available for the post processing, since the electronic and the software can handle
12 one 4096-bin spectrum every 30ms for an indefinite-long acquisition. The Mn_K α energy
13 resolution is below 130eV for 100kcps input-rate using 1 μ s filtering peaking-time. The system can
14 reach a count-rate up to 1Mcps input-rate using 400ns of peaking-time with a resolution <140eV at
15 Mn_K α . Peak to background ratio is typically greater than 15000.

16
17
18 The system is driven by an integrated controller board and an embedded PC with Ethernet or
19 wireless connection to the external computer. Three X-ray tube pine-hole collimators of 0.5mm, 1
20 mm and 2mm diameter are software selectable in order to obtain different spot-sizes on the sample.
21 A filter-set (with four software-selectable filters) is also integrated in the instrument head to
22 improve the detection limit in special applications. The design of the spectrometer allows the
23 detection of elements ranging from Na to U with good efficiency even in the region between 1 and
24 2keV (i.e. Na, Mg, Al, Si, P K-edge emissions) and in the region above 25keV (e.g. Sn, Sb, Ba K-
25 edge emissions). Na and Mg sensitivity can be improved further by purging Helium through a valve
26 integrated into the detection unit.

27
28
29 The XRF head is mounted on motorized stages that allow up to 60 \times 45cm² scanning area and 7,5cm
30 focusing axis. The system operates in non-contact mode with about 1 cm of distance from the
31 analysed object. The head is equipped with two lasers used to obtain the optimal working distance
32 and to check for the correct alignment of the scanning plane with respect to the sample surface. The
33 area under analysis can be monitored in real-time by the operator thanks to a microscope camera
34 (with dimming illumination adjustment) and an external camera with a larger field of view, both
35 integrated into the measurement head.

36
37
38 Thanks to a proper design of the mechanics, of the electronics and of the XRF components, the
39 scanning of the sample can be performed with a maximum speed up to 45mm/s. On-the-fly spectra
40 acquisitions with dwell time down to 30ms allow the scanner to perform fast and high-spatial
41 resolution measurements. The typical measurement time ranges from few tens of minutes up to few
42 hours depending on required spatial resolution, scanned area and contrast in the XRF maps. For
43
44
45
46
47
48
49
50
51
52
53
54
55
56
57
58
59
60

1
2
3 example the full scanned area ($45 \times 60 \text{cm}^2$) takes about 1h with the 2mm collimator and about 16h
4 with the 0.5mm collimator using a dwell time of 50ms.

5
6 The scanner can be mounted on a light trolley (see Fig.1) that enables the tilting of the motorized
7 frame between -90° and $+110^\circ$ with respect to the horizontal plane and height coarse regulation
8 (from 120cm up to 220cm) of the measured area. The overall weight of CRONO (including trolley,
9 motorized frame, and measurement head) is about 60kg, therefore it can be transported completely
10 assembled. Nevertheless, if necessary, the motorized frame and the trolley can be easily dismantled
11 for transportation to difficult sites. This is the case of archaeological sites, scaffoldings or
12 uncomfortable historical buildings for which CRONO can be profitably turned into a portable spot-
13 XRF device by simply detaching the measurement head from the motorized frame whenever
14 mapping is not necessary. The system is completed by an advanced software interface for the
15 complete instrument control, for data acquisition, for data analysis and to save raw data or prepare
16 in different format (including pdf files) final report documentation.
17
18
19
20
21
22
23
24

25 **Results and discussion**

26 **Analytical performances**

27
28 CRONO has been purposely designed for the use of pin-hole collimators instead of polycapillary
29 optics in order to make the system more suitable for analytical applications in heritage science. The
30 use of a polycapillary optics in MA-XRF instrumentation presents the advantage to have high
31 excitation photon flux when a small spot size (in the order of $100\mu\text{m}$ or below) is required. On the
32 other hand, a pin-hole collimator solution shows some remarkable advantages: (i) good sensitivity
33 over all elements even in the low energy region and for transitions in the range up to 35keV (e.g.
34 Sn, Sb, Ba K-edge emissions), (ii) very low divergence of the incident X-ray beam [2, 19] and
35 therefore low sensitivity to irregularities of sample's surface or misalignments that can degrade the
36 spot size uniformity over the sample, affecting the image quality, (iii) no need of expensive optics
37 and high power micro-focus tube with consequent cost effectiveness, (iv) possibility to design a
38 more compact and portable instrument.
39
40
41
42
43
44
45
46
47
48

49 The analytical sensitivity of CRONO was assessed on a NIST SRM610 glass standard with 500ppm
50 trace elements in a broad Z-range. Measurements were carried out at the operating conditions of
51 50kV, $200\mu\text{A}$, 1mm collimator, without X-ray filter and no He-purging (considered the reference
52 configuration). Fig.2 reports the spectrum acquired in 1000s with the identification of some
53 reference peaks. Fig.3a shows $K\alpha$ -line sensitivity in terms of counts per second (cps) of the net area
54 under the $K\alpha$ -line (processed with fitting algorithms implemented in the instrument software)
55 normalised to the certified concentration expressed in mg/g for the elements from $Z=19$ (K) to $Z=56$
56
57
58
59
60

1
2
3 (Ba): the measurement shows a good sensitivity (for a compact and portable instrument) both for
4 low-Z and high-Z elements. Considering the 1mm collimator, in the energy region around 3keV, for
5 instance, the sensitivity is above 40cps/(mg/g) for K; while in the energy region above 30keV the
6 sensitivity is above 100cps/(mg/g) for Ba. For elements in the intermediate range of $26 \leq Z \leq 47$ the
7 sensitivity reaches 1000-2000cps/(mg/g). Similar measurements were carried out using the 0.5mm
8 and 2mm collimators apertures available on CRONO. The results, presented in Fig.3a, show the
9 expected trend with the X-Ray flux hitting the sample: the sensitivity increases with larger
10 collimator and decreases with the smaller collimator. In order to validate the analytical sensitivity of
11 the instrument in conditions closer to the typical macro scanning operative ones, similar
12 measurements were performed with different acquisition time (1s, 10s and 100s) and with the
13 0.5mm collimator. The results are shown in Fig.3b. It is worth noting that, in tests with low
14 acquisition time and poor statistics due to the trace elements concentration (500ppm) of this
15 reference sample, the quality of the spectra fitting algorithm becomes crucial.

16
17
18
19
20
21
22
23
24 Fig.4 shows the limit of detection (LOD) calculated according to the standard definition [4],
25 measured with the same sample and in the same experimental conditions, in particular max tube
26 power (50kV, 200 μ A), 1mm collimator and 1000s of acquisition. In the energy region around 3keV
27 for instance the LOD is below 40ppm for K; while in the energy region above 30keV the LOD is
28 below 20ppm for Ba. For elements in the more sensitive intermediate range of $26 \leq Z \leq 47$ the LOD
29 is 1-2 ppm.

30
31
32
33
34 In order to test the spatial resolution capability of the scanner, the X-ray beam size at the optimum
35 focusing position (1cm from the sample) has been precisely determined with the knife-edge
36 technique performing dense scans of a thin metal sheet. The resulting data have been processed to
37 determine the X and Y dimension of the beam. The 0.5mm, 1mm and 2mm collimators produce a
38 beam size on the sample respectively of 0.85mm, 1.7mm and 3mm FWHM. It has also been
39 verified that the beam has almost circular geometry with about 10% ovalization.

40
41
42
43
44
45
46
47
48
49
50
51
52
53
54
55
56
57
58
59
60
The spatial resolution capabilities of CRONO have been confirmed on a reference standard with
several horizontal and vertical copper strips structures (line-pair per mm). The scan has been
performed at the maximum tube power settings (50kV and 200 μ A), horizontal motor speed of
4mm/s and dwell-time of 50ms per spectrum. The pixel dimensions of the reconstructed image are
250 \times 250 μ m² on the sample and the overall area is 95 \times 65mm². As shown in Fig.5, the 500 μ m
collimator aperture makes possible to discriminate one line-pair per mm in the lateral dimension
(that is 500 μ m detail discrimination). Further instrument developments are foreseen to reduce the
spot size on the sample, especially for applications that require higher spatial resolution. In
particular, preliminary studies regarding optimization of geometries of the X-ray collimator show

1
2
3 that a beam size on the sample of the order of 0.65mm with an estimated 40% reduction of the X-
4 ray flux can be implemented in the CRONO system.
5
6
7

8 **Example of application to a historical painting**

9
10 We benefited from potentials of CRONO for fast acquisitions of elemental distribution images to
11 assist the restorers of the “*Istituto Superiore per la Conservazione ed il Restauro-ISCR*” of Rome
12 during the restoration of a XV Century panel painting representing the *Virgin with the child* by an
13 unknown artist. The painting was damaged during a fire that deformed the wood panel and
14 blackened large part of the surface, as shown in the image of Fig.6. Preliminary point XRF analyses
15 performed by ISCR evidenced the permanence of the original pigments under the blackened layer.
16 Scanning XRF measurements were, therefore, considered necessary for a full characterization of the
17 elemental composition of the surface in order to provide information on the distribution of the
18 original pigments. Particular attention was focused on the recognition of the gilded areas in order to
19 preserve the remains of the gilding under the black layer during restoration.
20
21

22 Fig.6 reports some of the most informative elemental distribution images (Pb_L α , Hg_L α , Cu_K α ,
23 Au_L α , Fe_K and Ca_K α) recorded on a total scanned area of 46 \times 58cm² in three different
24 measurements with the following conditions: tube settings 50kV and 200 μ A, 2mm collimator
25 aperture, scanning speed of 19mm/s, dwell-time per pixel 100ms. Total measurement time was
26 about 2.5h. The elemental XRF maps were obtained by a standard *region of interest* (ROI) analysis
27 since more complex data elaboration is beyond the aim of this paper, being the authors more
28 focused on the presentation of the instrument capabilities. Due to the pronounced distortion of the
29 wood panel, the elemental distribution images present some mismatch between the overlapping
30 scanned areas. Nevertheless, the use of a pin-hole collimator allowed mitigating the artefacts due to
31 the unevenness of the surface and therefore good quality images have been obtained. They are
32 shown in Fig.6 and enable to appreciate significant details of the painting technique. For example
33 the Pb map suggests the use of the white pigment lead white (lead carbonate/hydrate lead
34 carbonate) for the flesh tones, revealing the face expression of the two figures, otherwise
35 completely indiscernible to the human eyes. Lead white has been also used for the drape around the
36 hips of the Child and it clearly appears in the Pb map to be fold and held by the Virgin's left hand
37 from where it falls down. Furthermore, the diffuse distribution of lead - especially in the gilded
38 background around the two saint figures - hints towards the presence of a preparatory white layer
39 (*imprimitura*) containing again lead white. The Hg map reveals the use of cinnabar (HgS) for the
40 darker highlights of the flesh tones of the two faces and of the Child's body. Cinnabar has also been
41 used for the vest of the Virgin together with iron (see Fe map), but only few remains of the pigment
42
43
44
45
46
47
48
49
50
51
52
53
54
55
56
57
58
59
60

1
2
3 are left and still visible only by MA-XRF. The Cu map clearly shows the use of a copper-based
4 pigment (most probably azurite, a blue basic copper carbonate) for the mantle of the Virgin.
5 Interestingly, in the internal side of the mantle the copper distribution reveals a fine floral
6 decoration which is also visible in the Fe and, with much lower intensity, in the Au maps, but as
7 negative images. In a similar way Fe looks more intense at the edges of the blue mantle around the
8 Virgin's figure. This fact can be ascribed to the use of bole (a red clay rich in iron) above the blue
9 layer as a preparation for the application of gold in order to produce a warmer colour. The Au
10 distribution image also reveals the technical choice of the artist to use gold foils for the background
11 gilding. In fact, especially on the right part of the gilded background, squared profiles with
12 increased intensity are clearly visible and ascribable to the overlapping of the gold leafs at the
13 boundaries. Besides to the gilded areas, iron is also present in the flesh and the hairs of the two
14 figures as well as in the red vest of the Virgin, suggesting the use of ochres (natural clays rich in
15 iron) as brown-red pigments. The same pattern of Fe is followed by the distribution of Ca, as this
16 latter is always present in clays. Furthermore, since Ca is the principal element of the grounds
17 (usually gypsum and glue), it can be used as indicator of the presence of missing paint areas
18 (*lacunas*), here mainly observed in the gilded background.
19
20
21
22
23
24
25
26
27
28
29
30
31
32
33
34
35
36
37
38
39
40
41
42
43
44
45
46
47
48
49
50
51
52
53
54
55
56
57
58
59
60

Conclusions

In this paper the recent development of the portable macro X-ray fluorescence (MA-XRF) scanner CRONO and its complete characterization in terms of detection sensitivity, spectroscopic and spatial resolution performances has been presented. The system has been designed with the aim of fulfilling specific analytical requirements for *in-situ* MA-XRF investigations of polychrome surfaces on heritage objects, i.e.: high sensitivity, good spatial resolution, large scanning areas, high scanning speed, portability, and easy re-configurability. In order to demonstrate the instrument capabilities for applications in the field of cultural heritage, the results from the study of a XV Century panel painting representing the *Virgin with the child* have been presented and discussed. The study was motivated by the presence of a diffuse blackened layer over the original paint produced by a past fire that prevents the visual reading of the painting and inhibits the work of restorers. Among the results provided by the MA-XRF investigation, the good resolution of the Ca, Fe and Au distribution images here presented allowed the restorers to trace in detail the distribution of the original gilding of the background under the black layer. Furthermore, MA-XRF revealed on the blue mantle of the Virgin a gold floral motif which is no longer visible. Nevertheless, the information on its original appearance is still preserved by the Fe and Cu distribution maps.

The successful use of CRONO to investigate an ancient painting as challenging case study not only demonstrates its diagnostic potentials in heritage science but also paves the way for applications in other fields demanding for high analytical performances in elemental analysis, such as industrial processes and material research in general.

Acknowledgements

We gratefully acknowledge for financial support of the national research projects SICH (PRIN 2010–2011 program) and FUTURAHMA (Future in Research - 2012 program), both funded by the Italian Ministry of Education, University and Research (MIUR).

Caption to figures

Fig.1: Crono XRF detection head mounted on the motorized frame and trolley in some of the possible configurations (vertical, horizontal, only the frame on the floor).

Fig.2: Spectrum of NIST SRM610 glass standard with 500ppm trace elements in a broad Z-range. Measurement conditions: 50kV, 200 μ A, 1mm collimator, 1000s, no filter and air atmosphere. Some reference peaks are identified.

Fig.3: (a) Measured sensitivity in counts per second per (mg/g) concentration for the elements from Z=19 (K) to Z=56 (Ba) and 2mm, 1mm and 0.5mm primary beam collimators. (b) same measurements with 1s, 10s and 100s and the 0.5mm collimator.

Fig.4: Limit of detection (LOD) for the elements from Z=19 (K) to Z=56 (Ba). X-ray tube operated at 50kV and 200 μ A, 1mm collimator and 1000s of acquisition.

Fig.5: Cu map from a scan of a reference standard with several horizontal and vertical copper strips structures (line-pair per mm). Conditions: X-ray tube settings 50kV and 200 μ A, no filter, air atmosphere, horizontal motor speed of 4mm/s, acquisition time 50ms per pixel, image reconstruction pixel dimensions 250 \times 250 μ m², overall area 95 \times 65 mm².

Fig.6: Far Left: Visible image of the painting "*Virgin with the child*" (XV Century) and evidenced scanned area in white line. Clockwise from middle-top: XRF elemental distribution maps of Pb_L α , Hg_L α , Cu_K α , Ca_K α , Au_L α and Fe_K α .

References

- [1] A. Longoni, C. Fiorini, P. Lautenegger, S. Sciutti, G. Fronterotta, L. Struder, P. Lechner, *Nuclear Instruments and Methods in Physics Research A*, 1998, 409, 407-409
- [2] M. Alfeld, K. Janssens, J. Dik, W. De Nolf, G. Van der Snickt, *J. Anal. At. Spectrom.*, 2011, 26, 899
- [3] F.-P. Hocquet, H. Calvo del Castillo, A. Cervera Xicotencatl, C. Bourgeois, C. Oger, A. Marchal, M. Clar, S. Rakkaa, E. Micha, D. Strivay, *Anal Bioanal Chem*, 2011, 399, 3109–3116
- [4] M. Alfeld, J. Vaz Pedroso, M. van Eikema Hommes, G. Van der Snickt, G. Tauber, J. Blaas, M. Haschke, K. Erler, J. Dik, K. Janssens, *J. Anal. At. Spectrom.*, 2013, 28, 760.
- [5] E. Ravaud, L. Pichon, E. Laval, V. Gonzalez, M. Eveno, T. Calligaro, *Appl. Phys. A*, 2016, 122, 17.
- [6] M. Alfeld, J.A.C. Broekaert, *Spectrochim. Acta Part B*, 2013, 88, 211
- [7] K. A. Dooley, D. M. Conover, L. Deming Glinsman, J. K. Delaney, *Angew. Chem.* 2014, 126, 13995 –13999
- [8] G. Van der Snickt, A. Martins, J. Delaney, K. Janssens, J. Zeibel, M. Duffy, C. McGlinchey, B. Van Driel, J. Dik, *Appl Spectrosc* 2016, 70, 57-67
- [9] M. Alfeld, G. Van der Snickt, F. Vanmeert, K. Janssens, J. Dik, K. Appel, L. van der Loeff, M. Chavannes, T. Meedendorp, E. Hendriks, *Appl Phys A*, 2013, 111, 165-175
- [10] K. Janssens, M. Alfeld, G. Van der Snickt, W. De Nolf, F. Vanmeert, M. Radepon, L. Monico, J. Dik, M. Cotte, G. Falkenberg, C. Miliani, B.G. Brunetti, *Annual Review of Analytical Chemistry*, 2013, 6, 399-425 .
- [11] D. Thurrowgood, D. Paterson, M. D. de Jonge, R. Kirkham, S. Thurrowgood, Daryl L. Howard, *Scientific Reports*, 2016, 6:29594, DOI: 10.1038/srep29594
- [12] M. Alfeld, W. De Nolf, S. Cagno, K. Appel, D.P. Siddons, A. Kuczewski, K. Janssens, J. Dik, K. Trentelman, M. Waltone, A. Sartorius, *J. Anal. At. Spectrom.*, 2013, 28, 40

- 1
2
3 [13] A. Martins, C. Albertson, C. McGlinchey, J. Dik, *Herit Sci* (2016) 4:22.
4
5
6 [14] K. Trentelman, M. Bouchard, M. Ganio, C. Namowicz, C. Schmidt Patterson, M. Walton,
7 X-Ray Spectrom. 2010, 39, 159–166
8
9
10 [15] F.P. Romano, C. Caliri, L. Cosentino, S. Gammino, L. Giuntini, D. Mascali, L. Neri, L.
11 Pappalardo, F. Rizzo, F. Taccetti, *Anal. Chem.* 2014, 86, 10892–10899.
12
13
14 [16] C. Miliari, F. Rosi, B.G. Brunetti, A. Sgamellotti, *Accounts of Chemical Research* 2010, 43,
15 728-738.
16
17
18 [17] L. Bombelli, C. Fiorini, T. Frizzi, R. Alberti and R. Quaglia, *IEEE Nucl. Sci. Symp. Med.*
19 *Imag. Conf. Rec. (NSS/MIC)*, 2012, pp. 418–420.
20
21
22 [18] <http://www.xglab.it/digital-pulse-processor-for-ultra-fast-detection-systems.shtml>
23
24
25 [19] K. Proost, L. Vincze, K. Janssens, N. Gao, E. Bulska, M. Schreiner and G. Falkenberg, *X-*
26 *Ray Spectrom.*, 2003, 32, 215–222
27
28
29
30
31
32
33
34
35
36
37
38
39
40
41
42
43
44
45
46
47
48
49
50
51
52
53
54
55
56
57
58
59
60

1
2
3
4
5
6
7
8
9
10
11
12
13
14
15
16
17
18
19
20
21
22
23
24
25
26
27
28
29
30
31
32
33
34
35
36
37
38
39
40
41
42
43
44
45
46
47
48
49
50
51
52
53
54
55
56
57
58
59
60



Fig.1: Crono XRF detection head mounted on the motorized frame and trolley in some of the possible configurations (vertical, horizontal, only the frame on the floor).

Fig.1
218x168mm (300 x 300 DPI)

view

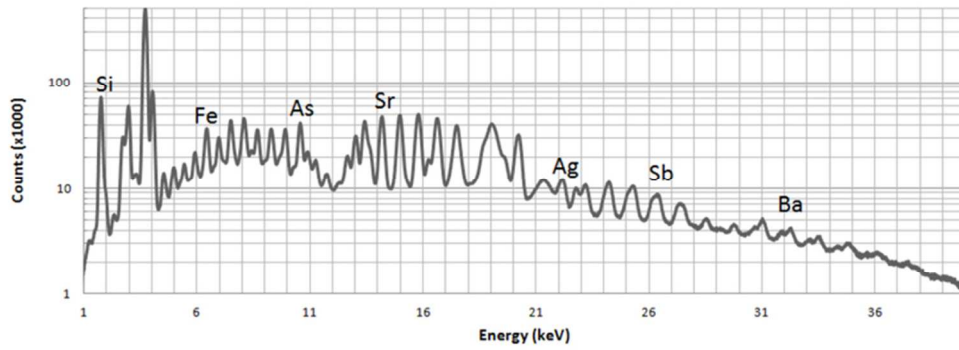


Fig.2: Spectrum of NIST SRM610 glass standard with 500ppm trace elements in a broad Z-range. Measurement conditions: 50kV, 200 μ A, 1mm collimator, 1000s, no filter and air atmosphere. Some reference peaks are identified.

Fig.2

35x13mm (600 x 600 DPI)

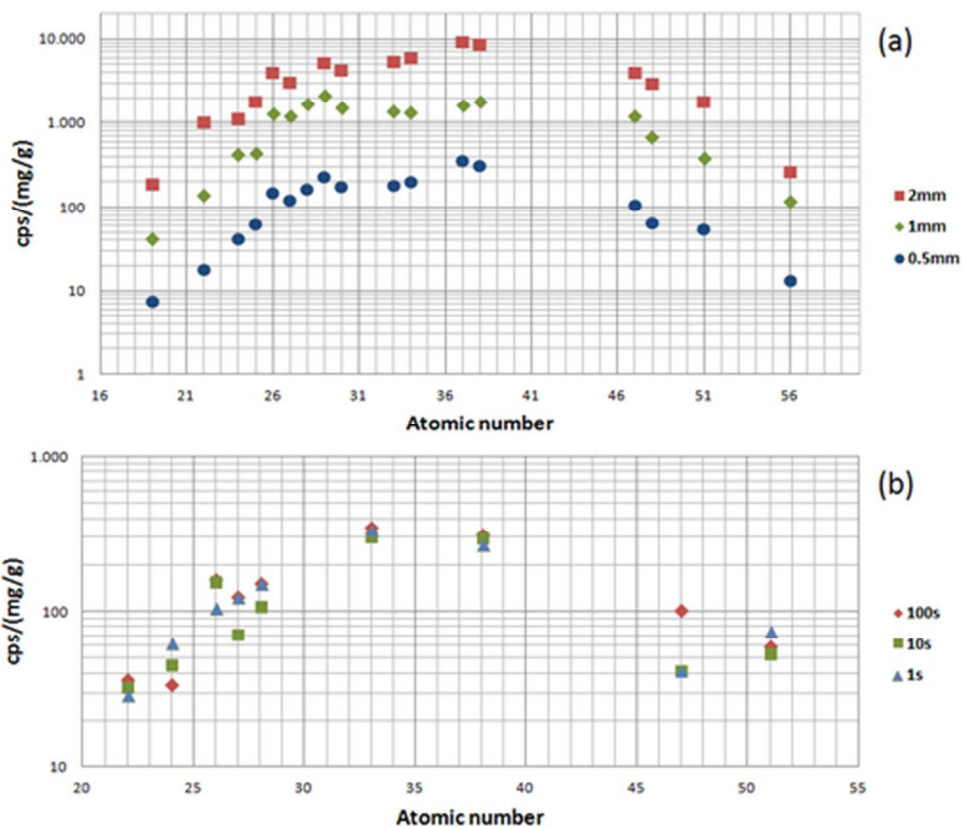


Fig.3: (a) Measured sensitivity in counts per second per (mg/g) concentration for the elements from Z=19 (K) to Z=56 (Ba) and 2mm, 1mm and 0.5mm primary beam collimators. (b) same measurements with 1s, 10s and 100s and the 0.5mm collimator.

Fig.3

22x19mm (600 x 600 DPI)



1
2
3
4
5
6
7
8
9
10
11
12
13
14
15
16
17
18
19
20
21
22
23
24
25
26
27
28
29
30
31
32
33
34
35
36
37
38
39
40
41
42
43
44
45
46
47
48
49
50
51
52
53
54
55
56
57
58
59
60

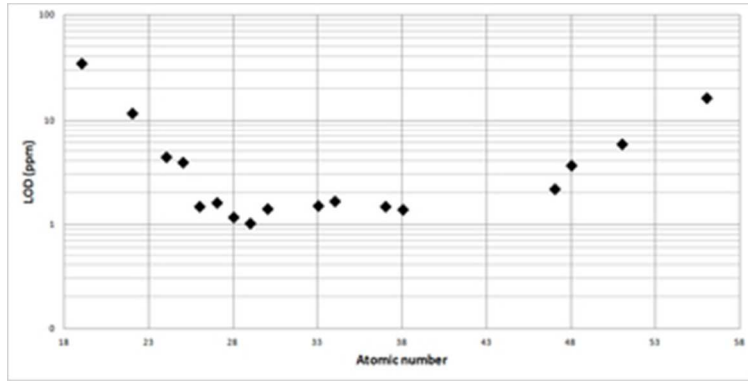


Fig.4: Limit of detection (LOD) for the elements from Z=19 (K) to Z=56 (Ba). X-ray tube operated at 50kV and 200 μ A, 1mm collimator and 1000s of acquisition.

Fig.4
15x8mm (600 x 600 DPI)

Peer Review

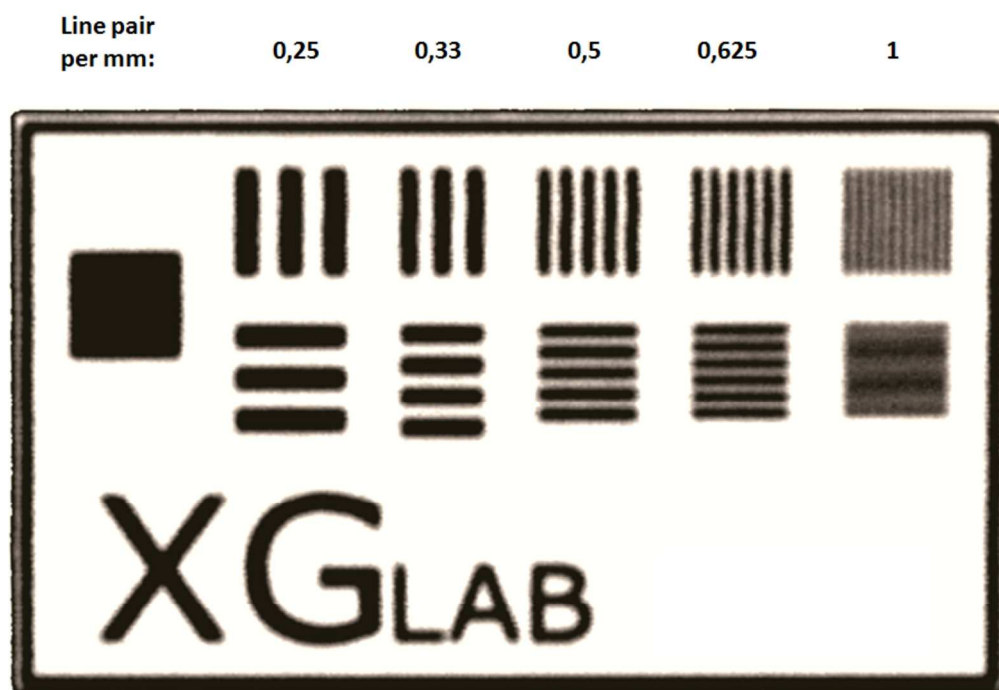


Fig.5: Cu map from a scan of a reference standard with several horizontal and vertical copper strips structures (line-pair per mm). Conditions: X-ray tube settings 50kV and 200uA, no filter, air atmosphere, horizontal motor speed of 4mm/s, acquisition time 50ms per pixel, image reconstruction pixel dimensions 250×250μm², overall area 95×65 mm².

Fig.5
169x119mm (300 x 300 DPI)

1
2
3
4
5
6
7
8
9
10
11
12
13
14
15
16
17
18
19
20
21
22
23
24
25
26
27
28
29
30
31
32
33
34
35
36
37
38
39
40
41
42
43
44
45
46
47
48
49
50
51
52
53
54
55
56
57
58
59
60

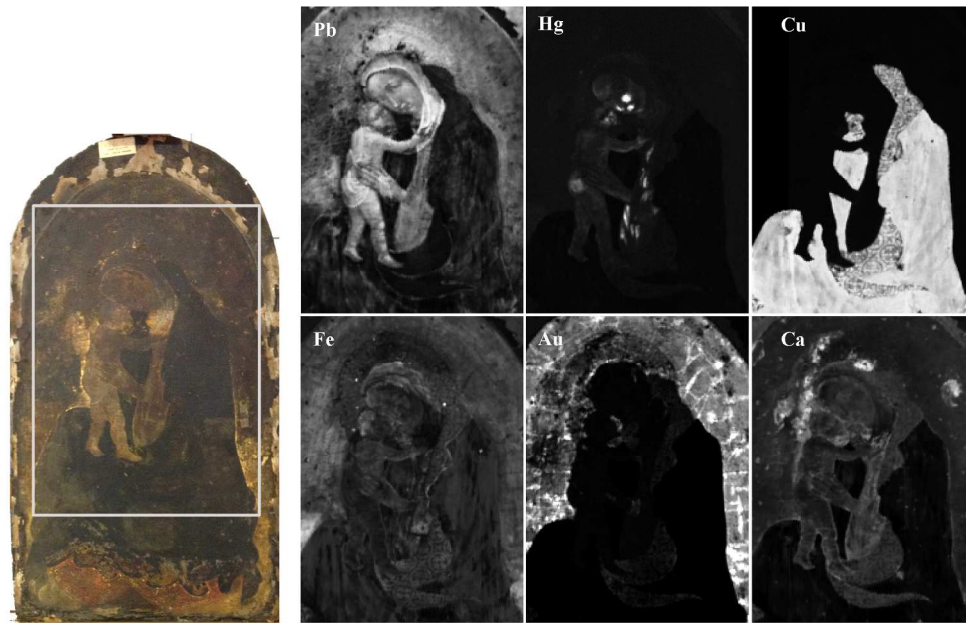


Fig.6: Far Left: Visible image of the painting "Virgin with the child" (XV Century) and evidenced scanned area in white line. Clockwise from middle-top: XRF elemental distribution maps of Pb_La, Hg_La, Cu_Ka, Ca_Ka, Au_La and Fe_Ka.

Fig.6
211x136mm (300 x 300 DPI)

Review